A simple model for voltage-dependent carrier collection efficiency in solar cells

R. F. McCarthy[1] and H. W. Hillhouse[2,a)]
[1]*School of Chemical Engineering, Purdue University, West Lafayette, Indiana 47907, USA*
[2]*Department of Chemical Engineering, University of Washington, Seattle, Washington 98195, USA*

(Received 6 November 2013; accepted 28 March 2014; published online 9 April 2014)

Here, we present a simple, yet powerful model developed to calculate collection efficiencies for photogenerated charge carriers in semiconductor devices. In the model, we define a new collection length, which is calculated using transit times that depend on both drift and diffusion for charge collection. The model accounts for a non-uniform electric field determined by the depletion approximation. The voltage-dependence of the photocurrent can be calculated using appropriate given photogeneration rate, and our results were found to match very closely with those calculated using a finite difference solution of the full device equations. The transit time model reported here leads to fully analytical equations for the collection length. They allow one to quickly explore wide ranges of parameters including mobility, minority carrier lifetime, and device thickness. The simplicity of this model allows it to be applied to other devices architectures as well. In fact, the motivating factor to develop the model was to quickly illuminate the advantages and disadvantages of various device designs, from nanostructured photovoltaics to light trapping strategies, and plasmonic enhancements. © *2014 AIP Publishing LLC*. [http://dx.doi.org/10.1063/1.4870827]

I. INTRODUCTION

One of the simplest models of photovoltaic device efficiency results from the "principle of the detailed balance" and was used by Shockley and Queisser[1] to provide an upper limit of the efficiency of a solar cell. This model ignores the inner workings of the solar cell and instead considers only the absorption and emission of photons. As a result, the model assumes radiative recombination as the only recombination pathway. Despite its simplicity, detailed balance models (variations of the original Shockley-Queisser calculation) are extremely useful for revealing the maximum theoretical efficiency of a solar cell given the bandgap (or bandgaps for multijunction devices), cell operating temperature, condition at the back surface (i.e., perfect reflector or a surface for radiative emission), and the illumination spectrum (i.e., blackbody spectrum, experimental AM1.5 GT, concentration, etc.). As a result, there is not one definitive "Shockley-Queisser limit," but a number of limits that depend on the constraints considered in the detailed balance (what can be absorbed and what can be emitted). However, almost all real devices have significant non-radiative recombination (the notable exception being high performance GaAs devices) that leads to decreased photocurrent and voltage. The focus of this paper is on more realistic (but still simple) models for photocurrent.

One widely used approach is to define a collection length or collection efficiency that can quickly estimate the photocurrent when other recombination pathways are present. Several models have been reported that account for different transport and recombination mechanisms. A few notable models summarized:

1. Common diffusion length. The most commonly encounter definitions for a collection length and collection efficiency are based on the diffusion only and are given as follows for a planar device:

$$L_{Dn} = \sqrt{\tau_n D_n}, \tag{1}$$

$$\eta_{C,D} = \exp\left(-\frac{(L-x)}{L_{Dn}}\right), \tag{2}$$

where τ_n is the effective minority carrier lifetime for electrons, D_n is the diffusion coefficient (based on the mobility) of an electron, x is position in the device, and L is the length of the device. Note that $\eta_{C,D}$ assumes total collection at the junction ($x = L$) and approaches zero at the end of the device ($x = 0$). The effects of Shockley-Read-Hall recombination or Auger recombination are imbedded in τ_n. However, the diffusion length accounts only for diffusive transport in the region where light is absorbed, mainly in the quasi-neutral region (QNR). This model is only applicable for thick solar cells like crystalline Si where the majority of the photons are absorbed in the QNR, or in extremely high efficiency devices where the diffusion length is larger than the cell thickness.
2. Hecht model for drift length. Hecht developed an equation for collection efficiency ($\eta_{C,H}$) that relied on a drift collection length ($L_{Drift,n}$ for electrons) given by

$$L_{Drift,n} = \mu_n \tau_n \vec{E}, \tag{3}$$

$$\eta_{C,H}(x) = \frac{L_{Drift,n}}{L}\left[1 - \exp\left(\frac{-x}{L_{Drift,n}}\right)\right], \tag{4}$$

where μ_n is the electron mobility and E is the electric field.[2] The electric field is assumed to be uniform for

a)Author to whom correspondence should be addressed. Electronic mail: h2@uw.edu

simplicity. This model works only for devices that have space-charge regions (SCR, where the electric field exists), but no QNR. Therefore, only transport caused by drift is accounted for. It was developed for semiconductor x-ray spectrometers and has also been applied to thin film devices that are fully depleted.

3. Crandall model. Crandall developed a similar model for studying a-Si p-i-n solar cells using drift collection lengths. However, Crandall expanded it further using the electron and hole continuity equations, and by accounting for recombination as well.[3,4] Limiting conditions for collection efficiency ($\eta_{C,C}$) under weakly absorbing light (Eq. (5a)) and strongly absorbing light (Eq. (5b)) are reported

$$\eta_{C,C} = \frac{L_{Drift}(V)}{L}, \tag{5a}$$

$$\eta_{C,C} = 1 - \frac{kT}{qL_A\vec{E}(V)}, \tag{5b}$$

where $L_{Drift}(V) = L_{Drift,n}(V) + L_{Drift,p}(V)$, k is Boltzmann's constant, T is the temperature of the device, q is the charge of an electron, and L_A is the photon absorption length. This model also uses a uniform electric field, but a voltage-dependent one. His photocurrent model was expanded on by Hegedus and used to study a-Si and a-SiGe p-i-n solar cells,[5] as well as CdTe/CdS devices (assuming low diffusion lengths).[6]

4. Other collection length models. A number of other collection length models also exist. Friedman developed a collection length for calculating depletion widths that depends on both the drift and diffusion collection lengths; however, this model does not apply in the QNR and still relies on a uniform electric field.[7,8] Crandall developed a much more complex model for thin film solar cells that does not assume a uniform field, but still is designed for the SCR.[9] Schiff reported a collection length for a-Si p-i-n solar cells that accounts for a non-uniform electric field, but works only for low mobility p-i-n cells with only radiative recombination and no diffusion.[10] None of the collection lengths discussed so far work well for typical thin film devices where there is both a quasi-neutral region and a depletion region, and charge is transported by both drift and diffusion.
5. Reciprocity theorem for collection efficiency. The reciprocity theorem states that the collection efficiency created by a photogenerated unit point charge is the same (with different dimensions) as the excess minority carrier distribution created by a unit point charge injection at the p-n junction under forward bias.[11,12] The carrier distribution can be easily calculated for a 1-D device using the minority carrier transport equations, and then Green's function allows for calculation of the collection efficiency. More complicated solutions are possible for 3 dimensional structures,[12–14] and it has even been applied to nanostructured photovoltaics.[15] However, there is a consistent limitation to this method. It can only be calculated in the quasi-neutral region, and requires a collection efficiency of unity in the depletion region. This limitation is problematic for very short minority carrier lifetimes or wide depletion widths where such an approximation is invalid.

Thus, there are no simple options to estimate the photocurrent for devices where both drift and diffusion are important. As a result, one must resort to numerical simulations of the coupled device equations for electrostatics and continuity. Software packages such as SCAPS, wxAMPS, and Sentaurus[16,17] are common, but simple 1D simulations can be solved by finite differences quite easily. While this approach is extremely useful for exploring the full details of device operation, they are not ideal for conceptual design or obtaining rough estimates. Here, we report the development of a new and simple collection efficiency model that can be used to estimate photocurrents of minority carrier based devices. The model accounts for charge transport via drift and diffusion, as well as recombination by Shockley-Read-Hall or other mechanisms described by an effective lifetime. We report a collection length, $\lambda_C(V)$, to describe the collection efficiency. $\lambda_C(V)$ is calculated by integrating the inverse charge carrier velocity, 1/v(x,V), across the device to yield a "transit time," t(x,V). The velocity accounts for diffusion and drift assuming a non-uniform electric field determined by the depletion approximation. $\lambda_C(V)$ is the distance from the junction to the point where $t(x,V) = \tau_n$, thus assuming that only charge with a transit time smaller than or equal to the minority carrier lifetime is collected. Our model results in a completely analytical equation for $\lambda_C(V)$. By ignoring other issues like reflection, contact resistance, and absorption by other semiconductors in the device, we obtain a simple but powerful model that accounts for the main recombination and transport mechanisms. We show that this model matches closely to results obtained using finite difference solutions. The simplicity of this collection efficiency will allow it to be easily adapted to different photovoltaics, such as light trapping devices, nanostructures, and plasmonics.

II. RESULTS AND DISCUSSIONS

A. Three key electrostatic regimes

Consider a simple 1-D structure with a p-type absorber layer (blue region) contacting a heavily doped n-type layer (yellow region), as seen in Figure 1. Since the n-type layer is heavily doped, we assume the depletion width in the n-type layer is approximately zero. Therefore, most of the band bending occurs within the p-type layer, and we can more easily calculate its depletion width ($W_P(V)$). The model works equally well if we assume an n-type absorber layer and heavily doped p-type layer. The equations for the electrostatics using the depletion approximation are given by

$$W_P(V) = \sqrt{\frac{2\,\varepsilon_S\,(V_{bi} - V)}{q\,N_A}}, \tag{6}$$

when $L > W_P(V)$

$$\vec{E}(x,V) = \begin{cases} -\frac{qN_A}{\varepsilon_S}(x - L + W_P(V)) & x \geq (L - W_P(V)) \\ 0 & x < (L - W_P(V)), \end{cases} \tag{7a}$$

and when $L \leq W_P(V)$

$$\vec{E}(x,V) = -\frac{qN_A}{\varepsilon_S}x, \tag{7b}$$

where ε_s is the dielectric constant, V_{bi} is the built-in-voltage, V is the applied voltage, and N_A is the acceptor concentration. There are three key electrostatic regimes, each of which depends on the thickness of the absorber layer, L. The first regime, we refer to as "QNR Dominated" (Fig. 1(a)). Here, L is much greater than $W_P(V)$, most of the film is within the QNR, and diffusion dominates charge transport. The second regime, we refer to as "SCR Dominated with Strong Fields" (Fig. 1(b)). L is approximately equal to $W_P(V)$, a large electric field exists over much of the film, and drift dominates charge transport. The final regime, we refer to as "SCR Dominated with Weak Fields" where L is much less than $W_P(V)$ (Fig. 1(c)). The films are so thin that the electric field cannot build up to a significant value, and diffusion dominates again.

B. Transit time model for voltage-dependent collection efficiency

To avoid invoking the full device equations (continuity equation and Poisson equation), we have developed what we refer to as a transit time model. In order to illustrate our approach, we first consider the case of diffusion only (no electric fields or drift). We simplify the calculation procedure by using a step-function for our collection efficiency (η_C(x)) that depends on our collection length (λ_C). η_C(x) has a value of 1 for a distance of λ_C from the junction, and a value of 0 beyond that (see Figure 2). We define λ_C as being proportional to L_{Dn}

$$\lambda_C = \beta L_{Dn}, \tag{8}$$

where β is a proportionality factor. If we simply set β equal to 1, then λ_C equals L_{Dn}. However, using this distance often overestimates the photocurrent as L_{Dn} reaches far out to the point where η_C(x) equals 0.368. Instead, we have chosen to define λ_C as the distance from the junction edge to the point where the diffusion model collection efficiency is 0.5, as depicted in Figure 2. Mathematically, we can set Eq. (2) to be equal to 0.5 at λ_C, and solving for β we get

$$\lambda_C = \beta L_{Dn} = \ln(2) L_{Dn}. \tag{9}$$

Another option for β is a term such that 50% of the area under the diffusion model curve is to the left and 50% to the right of λ_C, which comes from the following equation:

$$\lambda_C = \beta L_{Dn} = -\ln\left[0.5\left(1 + \exp\left(-\frac{L}{L_{Dn}}\right)\right)\right] L_{Dn}. \tag{10}$$

With this option, the transit time model solution for the photocurrent is exactly the same as the diffusion model when we have uniform generation. It also has an excellent approximation when the absorption profile is relatively flat. However, this term complicates the model, especially once drift is added in. For that reason, we have chosen to use ln(2) for β.

For our model, we define a characteristic carrier velocity. For the diffusion only case, and for reasons explained shortly, we choose to do so by dividing our collection length by τ_n (effective minority carrier lifetime),

$$\nu = \frac{\ln(2) L_{Dn}}{\tau_n}. \tag{11}$$

So in our diffusion-only model (a device with only a QNR), the characteristic velocity is constant and determined by τ_n and D_n. Consider a photogenerated minority carrier (an electron in the p-type layer) at a position, x. The electron diffuses towards

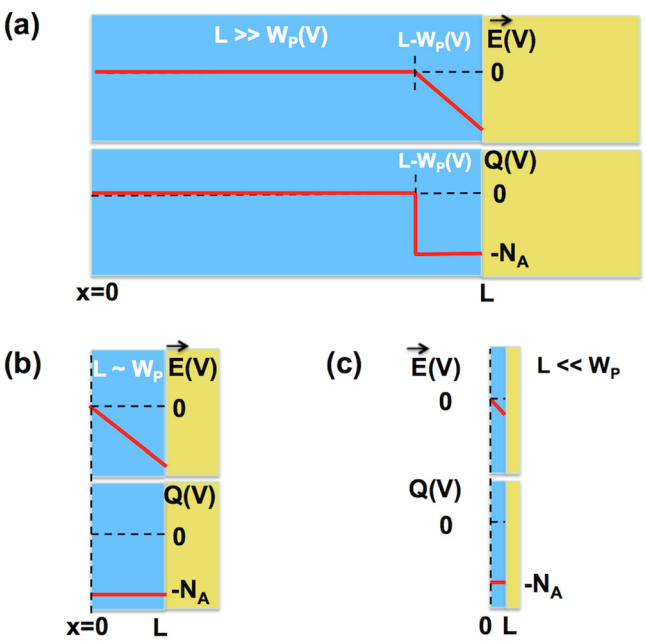

FIG. 1. Example models of thin film devices with a p-type absorber layer (blue region) and a heavily doped n-type layer (yellow region) for three different electrostatic regimes: Quasi-neutral region dominated where $L \gg W_P(V)$ (a); space-charge region dominated with strong fields where $L \sim W_P(V)$ (b); and space-charge region dominated with weak fields where $L \ll W_P(V)$ (c).

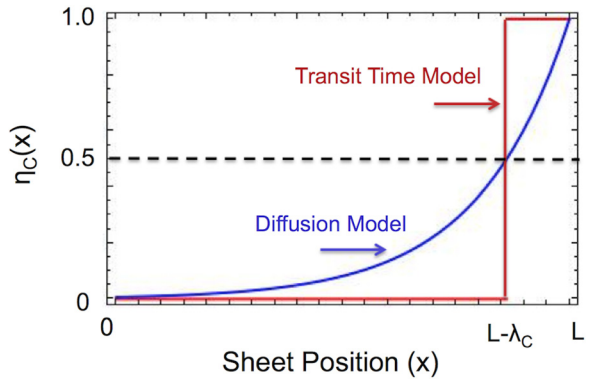

FIG. 2. A collection efficiency plot in the quasi-neutral region for the diffusion-only model (blue curve) and for our transit time model (red curve). The p-n junction is located at x = L.

the junction, and if it reaches the junction we assume it will contribute to the photocurrent. We define the transit time, t(x), to be the amount of time it takes the electron to reach the junction. We calculate this value by integrating 1/characteristic velocity from position x to the edge of the sheet,

$$t(x) = \int_x^L \frac{d\bar{x}}{\nu} = \frac{\tau_n}{\ln(2)\, L_{Dn}}(L - x). \tag{12}$$

What is the transit time for charge carriers that are one collection length from the junction edge? If we plug $L - \lambda_C$ in for x in Eq. (12), we find that $t(x) = \tau_n$. In choosing to divide λ_C by τ_n to calculate our velocity, we find that all charge carriers with lifetimes smaller than or equal to τ_n are collected and all others are not. In other words, we can also define λ_C as the point where $t(x) = \tau_n$. To calculate our photocurrent, we simply need to integrate the generation rate, g(x), multiplied by our collection efficiency. Since we have a step function for our collection efficiency, we need only integrate g(x) from the junction (the source of illumination) over the distance λ_C, or over the entire device if λ_C is longer than L

$$J_{Ph} = q \int_0^L g(x)\, \eta_C(x)\, dx, \tag{13a}$$

$$J_{Ph} = q \begin{cases} \displaystyle\int_{L-\lambda_C}^{L} g(x)\, dx & L > \lambda_C \\ \displaystyle\int_0^L g(x)\, dx & L \le \lambda_C, \end{cases} \tag{13b}$$

$$g(x) = \int_E \alpha(E)\, b_S \exp(-\alpha(E)\, x)\, dE, \tag{14}$$

where $\alpha(E)$ is the absorption coefficient and b_S is the incoming spectral flux.

So far the transit time model is very simple, but would only be valid for a device with no electric field. In order to account for the electric fields and drift transport, we go back to our characteristic velocity in Eq. (11) and add a term given by the drift collection length divided by τ_n

$$\nu(x, V) = \mu_n \vec{E}(x, V) + \ln(2)\, \frac{L_{Dn}}{\tau_n}. \tag{15}$$

Since we are using a non-uniform electric field determined by the depletion approximation, our velocity now has voltage and position dependence. Charge carriers both drift and diffuse to the junction, so the transit time also has voltage dependence now

$$t(x, V) = \int_x^L \frac{d\bar{x}}{\nu(\bar{x}, V)}. \tag{16}$$

Plugging Eqs. (6) and (7) into (15), and then solving (16), we obtain the following equations for t(x,V):

when $L > W_P(V)$ and $x \le L - W_P(V)$ (in the QNR)

$$t(x, V) = \frac{\varepsilon_S}{\mu_n q N_A} \ln\left(\frac{\frac{\mu_n q N_A}{\varepsilon_S} W_P(V) + \ln(2) \frac{L_{Dn}}{\tau_n}}{\ln(2) \frac{L_{Dn}}{\tau_n}} \right) + \frac{L - W_P(V) - x}{\ln(2) \frac{L_{Dn}}{\tau_n}}, \tag{17a}$$

when $L > W_P(V)$ and $x > L - W_P(V)$ (in the SCR)

$$t(x, V) = \frac{\varepsilon_S}{\mu_n q N_A} \ln\left(\frac{\frac{\mu_n q N_A}{\varepsilon_S} W_P(V) + \ln(2) \frac{L_{Dn}}{\tau_n}}{\frac{\mu_n q N_A}{\varepsilon_S} (x - L + W_P(V)) + \ln(2) \frac{L_{Dn}}{\tau_n}} \right), \tag{17b}$$

and when $L \le W_P(V)$ (device is fully depleted)

$$t(x, V) = \frac{\varepsilon_S}{\mu_n q N_A} \ln\left(\frac{\frac{\mu_n q N_A}{\varepsilon_S} L + \ln(2) \frac{L_{Dn}}{\tau_n}}{\frac{\mu_n q N_A}{\varepsilon_S} x + \ln(2) \frac{L_{Dn}}{\tau_n}} \right). \tag{17c}$$

Equation (17a) has two terms, the first accounting for time spent in the SCR and the second for time in the QNR. Since the velocity of a charge in the QNR is constant, the latter term is merely the ratio of the distance from charge generation to the SCR over the diffusion velocity. The SCR term depends on the natural log of the ratio of the maximum velocity ($x = L$ at the p-n junction) over the velocity at the edge of the SCR (diffusion velocity). There is also a constant term in front that depends inversely on the simplified form of Poisson's equation (qN_A/ε_S) and μ_n. Equation (17b) has no QNR term since the charge is generated in the SCR. The bottom term in the natural log ratio is now the velocity at the point of charge generation. Thus, as x approaches L the ratio approaches 1 and t(x,V) approaches 0. Equation (17c) is the same as (17b), but for very thin films where a smaller maximum velocity is achieved at the junction.

We will continue to define our now voltage-dependent collection length, $\lambda_c(V)$, as the distance from the junction to the point where the transit time is equal to τ_n. The relationship between $\lambda_c(V)$ and the spatially resolved collection efficiency, $\eta_c(x,V)$, is shown in Figure 3.

If we set each of Eqs. (17a)–(17c) equal to τ_n and then solve for x (which is $\lambda_c(V)$ in this case), we obtain the collection length

when $L > W_P(V)$ and $\lambda_c(V) \ge W_P(V)$

$$\lambda_C(V) = W_P(V) + \ln(2) L_{Dn} - \frac{\varepsilon_S}{\mu_n q N_A} \ln(2) \frac{L_{Dn}}{\tau_n} \ln\left(\frac{\frac{\mu_n q N_A}{\varepsilon_S} W_P(V) + \ln(2) \frac{L_{Dn}}{\tau_n}}{\ln(2) \frac{L_{Dn}}{\tau_n}} \right), \tag{18a}$$

when $L > W_P(V)$ and $\lambda_c(V) < W_P(V)$

$$\lambda_C(V) = W_P(V) - \frac{\varepsilon_S}{\mu_n q N_A}\left[\left(\frac{\mu_n q N_A}{\varepsilon_S} W_P(V) + \ln(2)\frac{L_{Dn}}{\tau_n}\right)\exp\left(\frac{-\tau_n}{\frac{\varepsilon_S}{\mu_n q N_A}}\right) - \ln(2)\frac{L_{Dn}}{\tau_n}\right], \tag{18b}$$

and when $L \leq W_P(V)$

$$\lambda_C(V) = L - \frac{\varepsilon_S}{\mu_n q N_A}\left[\left(\frac{\mu_n q N_A}{\varepsilon_S} L + \ln(2)\frac{L_{Dn}}{\tau_n}\right)\exp\left(\frac{-\tau_n}{\frac{\varepsilon_S}{\mu_n q N_A}}\right) - \ln(2)\frac{L_{Dn}}{\tau_n}\right]. \tag{18c}$$

Note that $\lambda_C(V)$ changes depending on whether the sheets are fully depleted and whether $\lambda_C(V)$ is located in the depletion region or not. Here we have developed a unique, simple, and analytical model for calculating voltage dependent collection efficiency.

Note: Unless otherwise stated, we assume for all example calculations below a semiconductor with band gap of 1.20 eV, a dielectric constant of 10.0, an electron effective mass of 0.1 m_e, a hole effective mass of 0.5m_e, and V_{bi} equals

$$V_{bi} = \frac{kT}{q}\left(\ln\left(\frac{N_C N_A}{n_i^2}\right) - (E_C - E_{F,n++})\right), \tag{19}$$

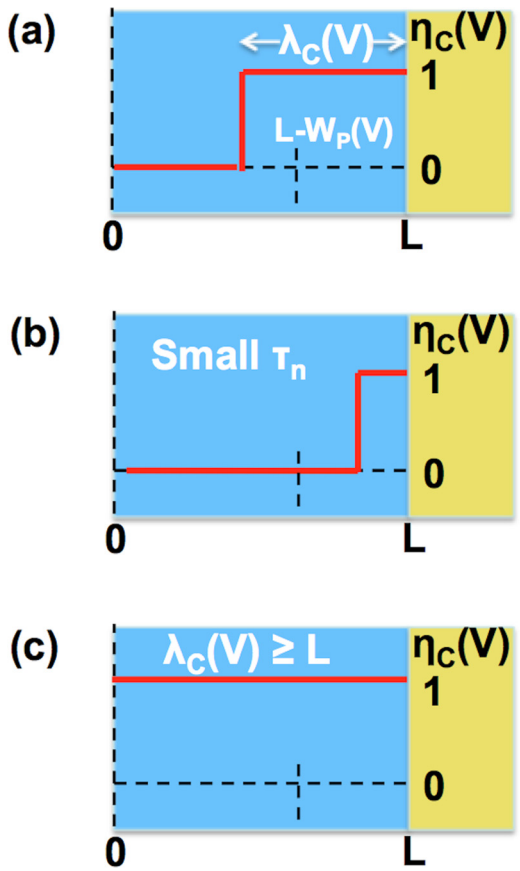

FIG. 3. Illustration of the connection between the collection length, $\lambda_C(V)$ and the spatially resolved collection efficiency, $\eta_c(x,V)$. (a) A case with SCR and QNR. (b) A case with very short minority carrier lifetime. (c) A case when $\lambda_C(V)$ is wider than the film.

where N_C is the effective conduction band density of states, E_C is the conduction band energy level, and $E_{F,n++}$ is the Fermi level of the n-type film. Note that $(E_C - E_{F,n++})$ was chosen such that when N_A is largest (just below degeneracy), V_{bi} equals the maximum possible V_{OC} as given by the Shockley-Queisser limit.

C. Comparison of the transit time model to finite difference solutions

Figure 4 compares collection efficiencies for various device thicknesses and electronic properties solved using two models: The transit time model and a finite difference model. The finite difference model calculates the electrostatics by solving Poisson's equation for a 1-D sheet using a variant of the nonlinear Poisson-Boltzmann Equation.[18] Using this electrostatics, the continuity equation for electrons was then solved using Eq. (20) with a delta function for the generation rate, g(x), at the position where the collection efficiency was calculated

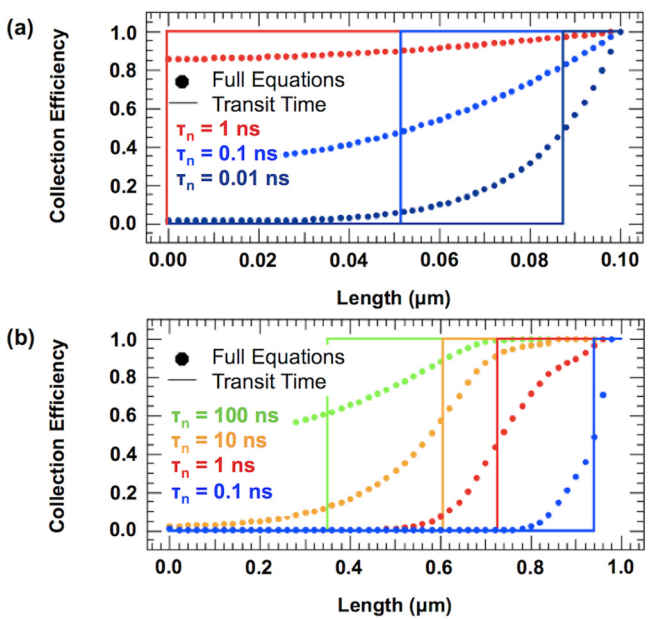

FIG. 4. The collection efficiency versus depth for various minority carrier lifetimes with $L = 0.1$ μm, $N_A = 10^{15}$ cm^{-3}, and $\mu_n = 10$ cm^2 V^{-1} s^{-1} (a) and $L = 1.0$ μm, $N_A = 10^{16}$ cm^{-3}, and $\mu_n = 1$ cm^2 V^{-1} s^{-1} (b). The junction is at the right of the figure ($x = L$).

$$D_n \frac{d^2\Delta n(x)}{dx^2} + \mu_n \vec{E}(x,V)\frac{d\Delta n(x)}{dx} + \mu_n \Delta n(x)\frac{d\vec{E}(x,V)}{dx} = \frac{n(x)\,p(x) - n_i^2}{\tau_n\,(n(x) + p(x) + 2\,n_i)} - g(x). \quad (20)$$

Here, we have assumed that the recombination is well modeled by a Shockley-Read-Hall mechanism with a mid-gap state and $\tau_n = \tau_p$.

Of course, our collection efficiency is only a step function while the finite difference solutions give a position dependent collection efficiency; however, we can see that even for different device thicknesses, doping concentrations, mobilities, and lifetimes (Figs. 4(a) and 4(b)) the area under the curve for the transit time model approximately equals that for the finite difference solutions. Though the position dependence of the transit time model's collection efficiency is unrealistic, its estimate for the amount of total photogenerated charge collected should be close to accurate.

D. Comparing short-circuit currents from the transit time model and full device equations

The importance of this model is of course dependent on its ability to predict photocurrents. We can use Eq. (13) the same as we did before except that we now have a voltage-dependent collection length that accounts for drift, which also makes our photocurrent voltage-dependent,

$$J_{Ph}(V) = q\int_0^L g(x)\,\eta_C(x,V)\,dx, \quad (21a)$$

$$J_{Ph}(V) = q\begin{cases} \displaystyle\int_{L-\lambda_C(V)}^{L} g(x)\,dx & L > \lambda_C(V) \\ \displaystyle\int_0^{L} g(x)\,dx & L \le \lambda_C(V). \end{cases} \quad (21b)$$

To calculate the photocurrent from finite difference equations, we again use Eq. (20) as solved by finite differences, but we use g(x) from Eq. (14) rather than delta functions. Results of these calculations are given in Figure 5, which shows the photocurrent (normalized to the maximum short-circuit current, $J_{SC,Max}$) as a function of voltage. For $N_A = 10^{15}$ cm^{-3} (Fig. 5(a)), the transit time model very closely matches the finite difference solutions. With strong electronic properties (yellow curve), the photocurrent stays flat since all generated charge is collected. Its value is less than one because the film is too thin (1 μm) to absorb the entire incoming spectrum. With shorter τ_n, the photocurrent starts to decrease at strong forward voltages due to the decreasing depletion width (red curve). The photocurrent drops even more quickly with a lower mobility (light blue curve). With a thinner film (0.1 μm), the photocurrent again stays flat due to the decreased distance to the junction (dark blue curve). However, the photocurrent is significantly decreased as less light is absorbed. If we have a carrier concentration of $N_A = 10^{16}$ cm^{-3} (Fig. 5(b)), the depletion width is shorter and charge collection decreases more quickly as the electronic properties worsen. This result is observed when comparing the red and light blue curves in Fig. 5(a) to Fig. 5(b) where fewer carriers are collected with the larger carrier concentration.

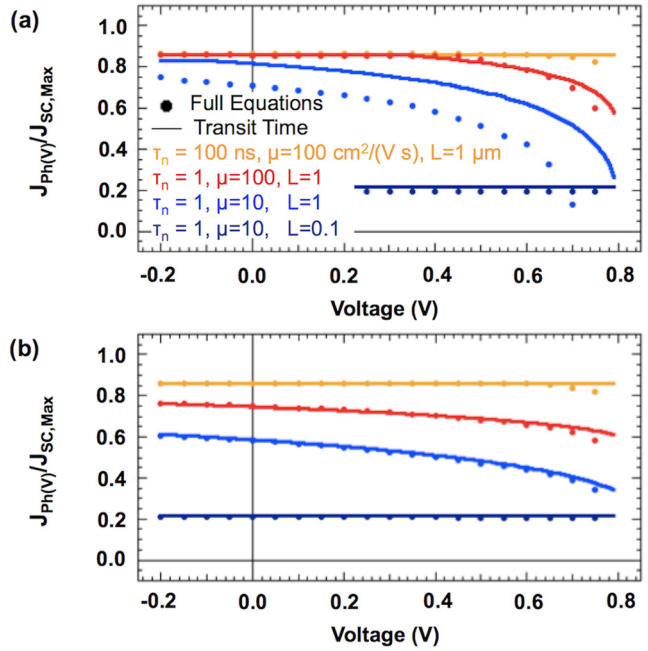

FIG. 5. Plots of $J_{Ph(V)}/J_{SC,Max}$ vs. V comparing the transit time model to finite difference solutions for various minority carrier lifetimes, mobilities, device thicknesses, and carrier concentrations of 10^{15} cm^{-3} (a) and 10^{16} cm^{-3} (b).

A plot of $J_{SC}/J_{SC,Max}$ vs. τ_n comparing our transit time model to the finite difference solutions is shown in Figure 6. For a thicker device (Fig. 6(a)), a large amount of current is possible for longer lifetimes, though an even thicker device would be required to reach full photon collection. The transit

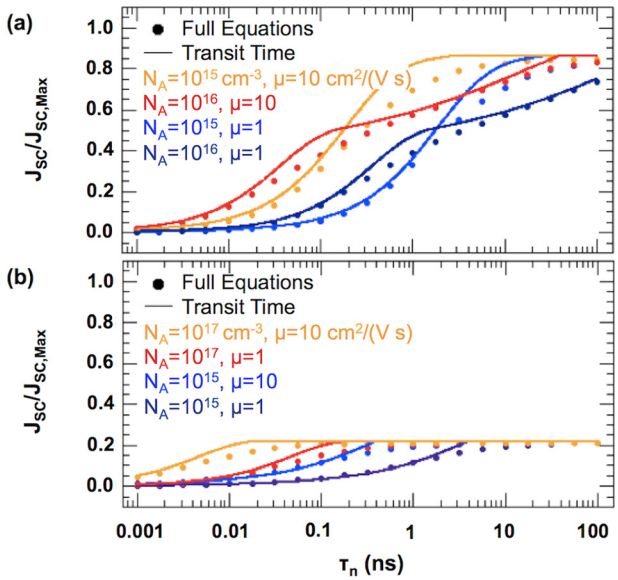

FIG. 6. Plots of $J_{SC}/J_{SC,Max}$ vs. τ_n comparing the transit time model to finite difference solutions for various carrier concentrations, mobilities, and device thicknesses of 1.0 μm (a) and 0.1 μm (b).

time model closely follows the finite difference solutions. There are a few discontinuities, such as near the center of Figure 6(a) for $N_A = 10^{16}$ cm^{-3} where the normalized J_{SC} decreases more slowly with τ_n because the electric field is resisting further loss of charge in the SCR. Though it is more pronounced for the transit model, these discontinuities also occur in the finite difference solutions. This discrepancy also explains the smaller photocurrent observed for the light blue curve in Fig. 5(a). Eventually, τ_n becomes small enough that even the electric field cannot help, and the current drops off quickly again. For thin devices (Fig. 6(b)), both models are greatly limited by the device thickness at long lifetimes. As τ_n begins to decrease, the finite difference solutions decrease shortly before the transit time model. However, it quickly catches up. Despite its simplicity, the transit time model follows closely.

Although less accurate for thin film devices where the majority of light is absorbed near the junction, one way to further simplify the photocurrent is by assuming a uniform generation rate (G) such that the photocurrent from the transit time model is simply given by

$$J_{Ph}(V) = \begin{cases} q\,\lambda_C(V)\,G & L > \lambda_C(V) \\ q\,L\,G & L \le \lambda_C(V). \end{cases} \quad (22)$$

Under this assumption, $J_{Ph}(V)$ is given by a simple but fully analytic set of equations. Though this assumption may not yield highly accurate results for planar devices, it's beneficial for showing how altering various electronic properties effects photocurrent without requiring numerical solutions. The assumption is more accurate for nanostructured devices and extremely thin absorbers (ETA) where very short distances separate generated charges from the junction. Over these short distances, generation is approximately uniform. A full nanostructure model utilizing the transit time model and the uniform generation assumption will be explored in another article.

This model does not account for some realistic problems such as reflectivity, shading by contacts, and absorption by other semiconductors in the device. It also assumes that the diffusion velocity is constant and equal to that in the QNR. However, these assumptions have allowed us to develop a simple photocurrent model utilizing a fully analytical collection length. This collection length accounts for a diffusion velocity and a drift velocity calculated using an electric field given by the depletion region. In this way, the main transport mechanisms are accounted for, allowing us to easily study a wide range of values for a number of different electronic parameters.

III. CONCLUSIONS

In this article, a simple model has been developed to calculate collection efficiencies for charge generation in semiconductor devices. The model is based on collection lengths, which are calculated by finding transit times for charge collection, which depend on both drift and diffusion. A voltage-dependent photocurrent can be calculated using a generation rate, and the results were found to match very closely with those calculated using finite difference solutions. These models lead to fully analytical equations for the collection length, and even the photocurrent when assuming average generation rates. The simplicity of this model will allow it to be applied to and, thus, illuminate other types of structures including nanostructured devices, light trapping material, and plasmonics.

ACKNOWLEDGMENTS

We would like to acknowledge support from the following organizations: Research Corp. for Science Advancement (Grant No. 20271), American Society for Engineering Education (NDSEG Fellowship, McCarthy), University of Washington, and the Washington STARS Program.

[1]W. Shockley and H. J. Queisser, J. Appl. Phys. **32**, 510 (1961).
[2]K. Hecht, Z. Phys. **77**, 235 (1932).
[3]R. S. Crandall, J. Appl. Phys. **53**, 3350 (1982).
[4]R. S. Crandall, J. Appl. Phys. **54**, 7176 (1983).
[5]S. S. Hegedus, Prog. Photovoltaics **5**, 151 (1997).
[6]S. Hegedus, D. Desai, and C. Thompson, Prog. Photovoltaics **15**, 587 (2007).
[7]M. Wolf, *Proc. IEEE* 51, 674 (1963).
[8]D. J. Friedman, A. J. Ptak, S. R. Kurtz, and J. F. Geisz, *Conference Record of the Thirty-First IEEE Photovoltaic Specialists Conference* (2005), p. 691.
[9]R. S. Crandall, J. Appl. Phys. **55**, 4418 (1984).
[10]E. A. Schiff, Sol. Energy Mater. Sol. Cells **78**, 567 (2003).
[11]C. Donolato, Appl. Phys. Lett. **46**, 270 (1985).
[12]K. Misiakos and F. A. Lindholm, J. Appl. Phys. **58**, 4743 (1985).
[13]T. Markvart, IEEE Trans. Electron Devices **44**, 1182 (1997).
[14]M. A. Green, J. Appl. Phys. **81**, 268 (1997).
[15]A. Wangperawong and S. F. Bent, Appl. Phys. Lett. **98**, 233106 (2011).
[16]M. Burgelman, P. Nollet, and S. Degrave, Thin Solid Films **361**, 527 (2000).
[17]Y. Liu, Y. Sun, and A. Rockett, Sol. Energy Mater. Sol. Cells **98**, 124 (2012).
[18]C. J. Nassar, J. F. Revelli, and R. J. Bowman, Commun. Nonlinear Sci. Numer. Simul. **16**, 2501 (2011).